Asymmetry in pulse-coupled oscillators with delay

M. Zeitler,[1,*] A. Daffertshofer,[2,†] and C. C. A. M. Gielen[1,‡]

[1]*Donders Institute for Brain, Cognition, and Behaviour, Radboud University Nijmegen,*
Geert Grooteplein 21, 6525 EZ Nijmegen, The Netherlands
[2]*Research Institute MOVE, VU University Amsterdam, van der Boechorststraat 9, 1081 BT Amsterdam, The Netherlands*

We studied the dynamics of synchronization in asymmetrically coupled neural oscillators with time delay. Stability analysis revealed that symmetric excitatory coupling results in synchrony at multiple phase relations. Asymmetry yields two saddle-node bifurcations of the stable states when coupling is asymmetric. By contrast, with inhibitory coupling only in phase or antiphase is stable as long as coupling is symmetric. Otherwise, these stable states shift or even vanish. The reduced bistability range suggests the beneficial role of asymmetric coupling for reliable neural information transfer.

Entrainment of weakly coupled nonlinear oscillators is well known for many years [1,2]. More recently, the synchronization dynamics in realistic settings received considerable interest, e.g., in nanomechanical oscillators [3], dynamic gene expression [4,5], and in neuronal networks [6–8], to mention a few. Interestingly, entrainment is believed to support information transfer in biological networks [9–12]. In this study, we discuss the emergence of and changes in synchronization between realistic neuronal systems described by nonlinear pulse-coupled oscillators [13,14]. Interaction between neurons is realized via changes in the membrane potential of a neuron due to the arrival of action potentials from another neuron at corresponding synapses. In several studies, neural systems were investigated in the case of symmetric coupling. Mirollo and Strogatz [14] provided a rigorous discussion of two pulse-coupled oscillators with symmetric excitatory connections and showed that they synchronize at zero phase difference. Ernst *et al.* [15,16] extended this study by introducing a time delay in the coupling due to finite conduction velocities of action potentials. The analytically derived return map of their model revealed that neurons with symmetric excitatory coupling synchronize at a phase lag equal to the delay, whereas in agreement with [17] inhibitory coupling results in stable in-phase synchronization, irrespective of the delay.

For two mutually connected neurons, the coupling strength from neuron 1 to neuron 2 can differ significantly from that from 2 to 1. Symmetrical coupling between neurons is indeed the exception rather than the rule. A previous study [18] has shown that a network of excitatory all-to-all pulse-coupled oscillators without delay but with slightly different coupling strengths always synchronizes, similar to the fully symmetric case in [14]. If time delays are introduced in a population of excitatory neurons with symmetric coupling, the network reveals emerging and decaying synchronized clusters [15]. For inhibitory coupling with time delays, the activity reveals synchronization in multistable clusters of common phases. A network with mainly inhibitory pulse-coupled oscillators with time delays and sparse coupling, which synchronizes for symmetric coupling strengths, desynchronizes when coupling strengths become asymmetric [19]. For increasing variation in the coupling strengths, the network state changes to an asynchronous aperiodic state. In the present study, we will investigate the stable states and the bifurcation diagram for two asymmetrically pulse-coupled oscillators with time delays for a large range of asymmetry in the coupling, both for excitatory and inhibitory couplings. To anticipate, the analytically derived bifurcation diagrams reveal distinct patterns of monostable and bistable states for asymmetric coupling and, more importantly, the present bifurcation routes. For the excitation, one of the states looses its stability and disappears; for the inhibition, the asymmetry shifts the in-phase and antiphase solutions to stable "out-of-phase" states.

Like Mirollo and Strogatz [14], we consider two oscillators with identical cycle period T and describe them by their phases ϕ_i with $d\phi_i/dt = 1/T$. Without loss of generality, we normalize the period to $T=1$. At $\phi_i=0$ oscillator, i is at its lowest state and at $\phi_i=1$, i.e., at the end of the cycle, the oscillator reaches threshold, emits a pulse, and resets its phase to zero. To cover a broad class of neuron models such as the leaky-integrate-and-fire neuron with fast synaptic responses or conductance-based threshold neurons [20], we describe the state of an oscillator by a smooth, monotonically increasing, and concave function $f:[0,1] \rightarrow [0,1]$ as in [14,15],

$$f(\phi) = b^{-1}\ln[1 + (e^b - 1)\phi]. \tag{1}$$

Since the neural oscillator is confined to $f(\phi)$, an input pulse yields a state change that is tantamount to a phase shift by a fixed amount depending on coupling type and strength. Two distinct shifts $\pm\varepsilon_{21}$ and $\pm\varepsilon_{12}$ have to be considered which reflect the coupling $1 \rightarrow 2$ and $2 \rightarrow 1$, respectively; the type of coupling, i.e., excitation or inhibition, determines whether the phase will be advanced ("+") or delayed ("−"), respectively. More formally, we use the updating rule for oscillator i [15,16],

$$\phi_{i,\text{new}}^{(\pm)} = \begin{cases} 1 \rightarrow 0 & \text{for} \quad 1 < f(\phi_i) + \varepsilon_{ij} \\ f^{-1}[f(\phi_i) \pm \varepsilon_{ij}] & \text{for} \quad 0 \leq f(\phi_i) \pm \varepsilon_{ij} \leq 1 \\ 0 & \text{for} \quad f(\phi_i) - \varepsilon_{ij} \leq 0. \end{cases} \tag{2}$$

*m.zeitler@science.ru.nl
†a.daffertshofer@fbw.vu.nl
‡s.gielen@science.ru.nl

If the oscillator receives a pulse at state $f(\phi_i) > 1 - \varepsilon_{ij}$, the phase shift immediately causes a pulse and a reset to phase zero ($\phi_{i,\text{new}}^+ = 1 \rightarrow 0$). Each input changes the phase of the oscillator and thereby the time of the next firing of the oscillator. The change in the time of the next action potential for input at various phases in the cycle of the oscillator relative to the period of the oscillator defines the phase response curve [21] of the Mirollo-Strogatz oscillator $\Delta^{(\pm)}[\phi_i] = \frac{T_{\text{new}} - T}{T} = \phi_{i,\text{new}}^{(\pm)} - \phi_i$. Positive (negative) values of this function correspond to phase advances (delays) in the sense that they advance (delay) the time of the next spike.

We assess stability of the system via the phase difference at times t_k at which oscillator 1 generates the kth pulse, i.e., $\Phi_k = \phi_2(t_k) - \phi_1(t_k)$. Because oscillator 1 fires and resets immediately, $\phi_1(t_k) \rightarrow 0$ holds, and we can simplify $\Phi_k = \phi_2(t_k)$. This stroboscopic view yields the system's return map $R[\Phi]$ with fixed points $R[\Phi^*] = \Phi^*$. To illustrate the subsequent stability classification [22], we briefly sketch the synchronization characteristics in the case of two excitatory couplings [14]; the inhibitory case can be treated equivalently. For instantaneous couplings, i.e., without finite conduction delays, three different regimes can be distinguished depending on the firing moments t_k and the $\Delta^{(+)}$. We note that here the latter is readily parametrized via the coupling strength ε_{ij} since we fixed b. In regime I, oscillator 1 receives a pulse from oscillator 2 late in its cycle and fires immediately, i.e., both are synchronized in phase. In regime II, 1 receives a pulse and returns it with a finite lag and so does 2, i.e., the system is synchronized out of phase. Finally, in regime III, oscillator 1 reacts with a certain lag but 2 does reply immediately yielding again in-phase synchronization. The corresponding return maps reveal that the synchronized states are stable in I and III but not in II. That is, the oscillators always synchronize with zero phase lag (in phase). Further, we incorporate a delay because the emitted pulse may arrive at the other oscillator after a finite time τ. With delay, an excitatory coupling results not in three but 14 different regimes. The corresponding return maps contain in total six fixed points, from which one half is asymptotically stable and the other half is unstable. The latter separate the attraction domains of the stable fixed points. Unlike the excitatory coupling, inhibition with delay results in marginally stable fixed points next to the asymptotically stable ones.

Figure 1 shows the fixed points of the return map as a function of coupling strengths ε_{ij} and delay τ; in all figures, we used $b = 3$. With symmetric coupling $\varepsilon_{21} = \varepsilon_{12} = \varepsilon$, two stable states coexist for small delay τ as shown in Fig. 1(B) (upper panel). One state is at $\Phi^* = \tau$ which implies that oscillator 2 drives 1, which in response, fires an action potential immediately after the arrival of the pulse. The other one is at $\Phi^* = 1 - \tau - \Delta^{(\pm)}[\phi_2(t_k + \tau)]$. The arrival of the τ-delayed pulse of oscillator 1 yields a phase shift $\Delta^{(\pm)}[\phi_2(t_k + \tau)] > 0$, which shortens the period of oscillator 2 to $T_{\text{new}} = 1 - \Delta^{(\pm)}[\phi_2(t_k + \tau)]$ and induces a pulse delayed by τ after 1 has fired. The resulting phase shift increases for larger delays because $\Delta^{(\pm)}[\phi_2(t_k + \tau)] = 2\tau[(1/\phi_{\text{crit}}^{(+)}) - 1]$; here, we abbreviated $\phi_{\text{crit}}^{(+)} = (e^{b(1-\varepsilon_{12})} - 1)/(e^b - 1)$ (see also the Appendix). The period of the coupled system hence decreases for increasing τ until it reaches $T_{\text{new}} = 2\tau$. For
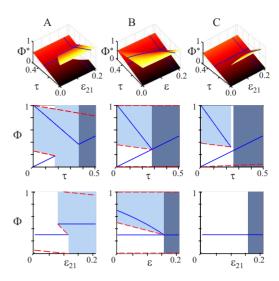

FIG. 1. (Color online) (Un-)stable states for two excitatory pulse-coupled oscillators with delay. (A) Asymmetric coupling with $\varepsilon_{12} = 0.1$. (B) Symmetric coupling with $\varepsilon_{21} = \varepsilon_{12} = \varepsilon$. (C) Asymmetric coupling with $\varepsilon_{12} = 0.2$. Top: asymptotically stable fixed points of the return map as a function of τ and ε_{21}. Solid lines represent the cross sections shown in middle and bottom rows. Middle: stable (blue, solid line) and unstable (red, dashed line) fixed points and their attraction domains as a function of τ for $\varepsilon_{21} = 0.18$. Bottom: same as the middle row as a function of coupling strength for $\tau = 0.3$.

larger values of τ, the period increases and only one stable state remains representing antiphase synchrony, i.e., $\Phi^* = 0.5 T_{\text{new}} = \tau$. At $\varepsilon = 1 - b^{-1} \ln[2\tau(e^b - 1) + 1]$, two stable states merge via a supercritical pitchfork bifurcation into a single stable state in which the neurons oscillate in antiphase [Fig. 1(B), middle and lower panels]. Put differently, in the absence of time delays, an excitatory coupling leads to in-phase synchronization [14], whereas a delay yields out-of-phase synchronization [16,17]. Note that the dynamics of synaptic connections, which is typically modeled via $(t/\tau_s^2)\exp\{-t/\tau_s\}$ may add to the here-discussed delay so that larger values of τ_s may contribute to the aforementioned supercritical pitchfork bifurcation from out-of-phase into antiphase synchrony [17]. The explicit form of that dynamics, however, does not alter the qualitative behavior of our system so that a pulselike coupling appears proper for the current discussion.

As soon as the synaptic coupling strengths differ ($\varepsilon_{12} \neq \varepsilon_{21}$), the pitchfork bifurcation is no longer present and the upper stable state $\Phi^* = T_{\text{new}} - \tau$ disappears for

$$\varepsilon_{21} < 1 - b^{-1} \ln\left[1 + (e^b - 1)\left(1 - \frac{2\tau(1 - \phi_{\text{crit}}^{(+)})}{\phi_{\text{crit}}^{(+)}}\right)\right], \quad (3)$$

e.g., in the lower panel of Fig. 1(A). That is, there is only one stable branch $\Phi^* = \tau$, in which oscillator 2 drives oscillator 1, which, in turn, disappears for

$$\varepsilon_{21} > 1 - b^{-1} \ln\left[1 + \frac{e^b - 1}{1 + \frac{1 - \phi_{\text{crit}}^{(+)}}{2\tau}}\right]. \quad (4)$$

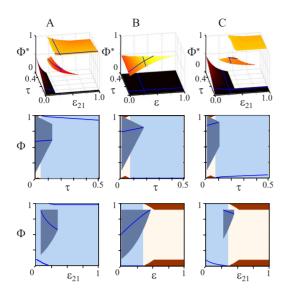Stable states and corresponding attraction domains are shown in the lower panel of Fig. 1(A) as a function of cou-

FIG. 2. (Color online) (Un-)stable states for two inhibitory pulse-coupled oscillators with delay. (A) Asymmetric case with $\varepsilon_{12}=0.2$. (B) Symmetric case: $\varepsilon_{21}=\varepsilon_{12}=\varepsilon$. (C) Asymmetric coupling with $\varepsilon_{12}=0.4$. Asymptotically stable fixed points Φ^* of the return map as a function of τ and ε_{21} [cf. Fig. 1 now with $\varepsilon_{21}=0.3$ (middle row) and $\tau=0.1$ (bottom row)].

pling strength ε_{21}. At a critical value $\varepsilon_{21}<\varepsilon_{12}$, the upper stable state merges with an unstable equilibrium through a saddle-node bifurcation and vanishes for smaller ε_{21}. For slightly larger coupling strength ε_{21}, the lower stable state merges with an unstable state. Figure 1(A) (middle panel) shows the corresponding stable and unstable states as a function of τ for $\varepsilon_{12}<\varepsilon_{21}$. For this asymmetry, the pitchfork bifurcation at $\varepsilon_{12}=\varepsilon_{21}$ (1B, middle panel) disappears and a saddle-node bifurcation emerges. The two excitatory coupled oscillators are precisely in antiphase if both coupling strengths ε_{ij} obey

$$\varepsilon_{ij} \geq 1 - b^{-1} \ln[2\tau(e^b-1)+1]. \tag{5}$$

From Fig. 1 and Eq. (5), we can conclude that only if $\varepsilon_{12}=\varepsilon_{21}=1-b^{-1}\ln[2\tau(e^b-1)+1]$, the two stable out-of-phase states will merge (in the antiphase state). The supercritical pitchfork bifurcation, which is characteristic for excitatory symmetrically pulse-coupled oscillators with delay, does not exist for asymmetric coupling and is replaced by two saddle-node bifurcations with two stable states, at least when the difference between the two coupling strengths is sufficiently small.

If coupling is inhibitory, the spectrum of solutions and bifurcations changes entirely. Figure 2(B) shows the results for inhibitory symmetrically pulse-coupled oscillators with delay. The in-phase synchronization $\Phi^*=0$ is a stable state for all coupling strengths and delays and a stable antiphase state exists for

$$\varepsilon \leq -b^{-1} \ln\left[\frac{2\tau-1}{1+\frac{1}{e^b-1}}+1\right] \tag{6}$$

[see upper surface in Fig. 2(B) (upper panel) and the cross section at fixed τ in the lower panel]. Since unstable states

are absent, the attraction domain of the antiphase solution is an open manifold. If the phase difference Φ lies on one of the two separatrices, here at

$$\Phi = 1 - \tau, \quad \Phi = (2e^{b\varepsilon}-1)\tau + \phi_{\text{crit}}^{(-)}, \tag{7}$$

it converges to the stable in-phase state or to the region of marginal stability $\{\varepsilon \geq b^{-1} \ln[\tau(e^b-1)+1]\}$. The cross section for fixed τ [Fig. 2(B), lower panel] shows that in-phase and antiphase states coexist for small ε and marginally stable states exist for large ε, which agrees with previous studies (e.g., [15]). In the middle and lower panels of Fig. 2(B), we find that one stable fixed point and two separatrices merge and vanish. This bifurcation occurs at

$$\varepsilon = -b^{-1} \ln\left[\frac{2\tau-1}{1+1/(e^b-1)}+1\right]. \tag{8}$$

If asymmetry is introduced to the inhibitory coupling, the in phase and antiphase do not remain stable [upper panels of Figs. 2(A) and 2(C)]. The stable state $\Phi^*=0$ changes to a stable phase difference near zero [middle and lower panels of Figs. 2(A) and 2(C)]. Similarly, a stable near antiphase state exists for a range of values for τ and ε being smaller than for the antiphase oscillation in the symmetrically coupled system. For $\varepsilon_{12}<\varepsilon_{21}$, this state merges with the lower separatrix for

$$\varepsilon_{21} = b^{-1} \ln\left[1 - \frac{e^{-b\varepsilon_{12}}-1}{e^{-b}+2\tau(1-e^{-b})}\right] \tag{9}$$

[see also the right-hand side of the stable state range in the middle panel of Fig. 2(A) and the lower panels of Figs. 2(A) and 2(C)]. Similarly, for $\varepsilon_{12}>\varepsilon_{21}$, the near antiphase state merges with the upper separatrix at

$$\varepsilon_{21} = -b^{-1} \ln[1 + \{1 - e^{b\varepsilon_{12}}[2\tau(1-e^{-b})+e^{-b}]\}] \tag{10}$$

[see the left-hand side of the stable state range in the lower panels of Figs. 2(A) and 2(C) and the right-hand side of the stable state range in the middle panel of Fig. 2(C)]. At $\Phi^*=0$, a degeneration to multiple stable states occurs if the minimum value of the actual coupling strengths equals $b^{-1} \ln[\tau(e^b-1)+1]$ [see middle panels of Figs. 2(A) and 2(C) and lower panel of Fig. 2(C)]. Notice that the dynamics of synapses, i.e., $(t/\tau_s^2)\exp\{-t/\tau_s\}$ in the inhibitory case with delay makes the marginally stable states disappear and causes the coexistence of stable in phase and antiphase states for all delays and coupling strengths as long as coupling is symmetric. For asymmetric coupling, two stable states coexist, which are not precisely in phase or antiphase.

Figure 3 summarizes the results for different values of τ. A system with two excitatory pulse-coupled oscillators with delay hence reveals monostability or bistability depending on ε_{12}, ε_{21}, and τ. At the transition from monostability to bistability, a saddle-node bifurcation is found. These two saddle-node bifurcations meet at the diagonal $\varepsilon_{12}=\varepsilon_{21}$ and combine into a supercritical pitchfork bifurcation.

Several studies have studied asymmetry in the coupling between excitatory oscillators. For small differences in mutual coupling strength, the results are qualitatively similar to that for symmetrical coupling [18]. In this study, we show
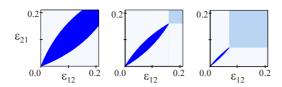
FIG. 3. (Color online) Number of stable states for two asymmetric pulse-coupled oscillators as function of excitatory coupling strengths $\tau=\{0.2,0.3,0.4\}$ (from left to right). The darkest areas correspond to bistability contrasting monostability outside this area. The square in the right upper corner of the middle and right panels represents the region where the two oscillators are in antiphase.

that two stable states merge into a single stable state, when the differences in coupling strengths increase. Networks with inhibitory pulse-coupled oscillators behave qualitatively different. Denker *et al.* [19] showed that a population of mainly inhibitory pulse-coupled oscillators desynchronizes if asymmetry in coupling strengths increases. In addition to Denker *et al.* [19], who started with a synchronized network which turns into a desynchronized state for asymmetric coupling, we find that both the in-phase and antiphase states become unstable.

Symmetrically and asymmetrically coupled oscillators show qualitatively different behavior of monostability/ bistability. Asymmetric excitatory coupling yields a bifurcation pattern in which two saddle-node bifurcations merge into a pitchfork bifurcation when switching to symmetry. For inhibitory coupled oscillators, two stable states are present corresponding to either in-phase or antiphase synchronization in the symmetric case or near in phase or antiphase for asymmetric coupling. In the latter case, stable states vanish by merging with a separatrix. When synaptic dynamics are incorporated, marginal stability vanishes and the symmetric inhibitory coupled system has two stable states for all coupling strengths and delays. Irrespective of the coupling type (excitatory or inhibitory, with or without synaptic dynamics), asymmetry generally leads to a smaller range of bistability as compared to its symmetric counterpart. A pronounced asymmetry in coupling hence supports the (directed) information exchange between neurons. Information is transmitted reliably in one direction since the receiving excitatory neuron will instantaneously emit a pulse after the arrival of the pulse from the sending neuron. The bifurcation diagrams show that the transfer of information is robust for fluctuations in coupling strength. Transmission is readily achieved since the receiving neuron is driven by the sending neuron and the phase relation between the neurons does not change in case of small changes in coupling strengths caused by the synaptic plasticity.

APPENDIX

The phase responsive curve of Mirollo and Strogatz showed always a phase advance even if the oscillator generates a pulse, which seems improper for realistic neurons. Hence, we corrected

$$\Delta^{(\pm)} = 1 - \phi + \begin{cases} \phi/\phi_{\text{crit}}^{(+)} - 1 & \text{for } \phi \leq \phi_{\text{crit}}^{(+)} \\ 0 & \text{otherwise,} \end{cases}$$

where $\phi_{\text{crit}}^{(+)} = (e^{b(1-\varepsilon)} - 1)/(e^b - 1)$ represents the phase at which the maximum shift is reached. When a pulse arrives at the oscillator at phase $\phi > \phi_{\text{crit}}^{(+)}$, the oscillator emits a pulse. For biological systems, the phase shift reaches its maximum when the input arrives in the second half of the cycle period (see [23]), i.e., $\phi_{\text{crit}}^{(+)} > 0.5$, yielding $\varepsilon \leq 0.21$. Similarly, for the inhibitory case, we used

$$\Delta^{(-)} = -\phi + \begin{cases} e^{-b\varepsilon}(\phi - \phi_{\text{crit}}^{(-)}) & \text{for } \phi > \phi_{\text{crit}}^{(-)} \\ 0 & \text{otherwise,} \end{cases}$$

with $\phi_{\text{crit}}^{(-)} = (e^{b\varepsilon} - 1)/(e^b - 1)$ and $\phi \in [0,1)$. Note that here the coupling is not bounded apart from $\varepsilon < 1$.

[1] Y. Kuramoto, *Chemical Oscillations, Waves and Turbulence* (Springer, New York, 1984).

[2] P. A. Tass, *Phase Resetting in Medicine and Biology* (Springer, New York, 1999).

[3] S. Shim *et al.*, Science **316**, 95 (2007).

[4] K. I. Mazzitello *et al.*, Phys. Rev. E **78**, 021906 (2008).

[5] K. Horikawa *et al.*, Nature (London) **441**, 719 (2006).

[6] V. Shusterman and W. C. Troy, Phys. Rev. E **77**, 061911 (2008).

[7] H. Câteau *et al.*, Phys. Rev. E **77**, 051909 (2008).

[8] D. Battaglia *et al.*, Phys. Rev. Lett. **99**, 238106 (2007).

[9] A. Winfree, *The Geometry of Biological Time* (Springer, New York, 1980).

[10] P. Fries, Trends Cogn. Sci. **9**, 474 (2005).

[11] A. Schnitzler and J. Gross, Nat. Rev. Neurosci. **6**, 285 (2005).

[12] R. T. Canolty *et al.*, Science **313**, 1626 (2006).

[13] H. Haken, *Brain Dynamics* (Springer, New York, 2008).

[14] R. Mirollo and S. Strogatz, SIAM J. Appl. Math. **50**, 1645 (1990).

[15] U. Ernst *et al.*, Phys. Rev. Lett. **74**, 1570 (1995).

[16] U. Ernst *et al.*, Phys. Rev. E **57**, 2150 (1998).

[17] C. Vreeswijk *et al.*, J. Comput. Neurosci. **1**, 313 (1994).

[18] W. Senn and R. Urbanczik, SIAM J. Appl. Math. **61**, 1143 (2000).

[19] M. Denker *et al.*, Phys. Rev. Lett. **92**, 074103 (2004).

[20] M. Timme *et al.*, Chaos **13**, 377 (2003).

[21] E. M. Izhikevich, *Dynamical Systems in Neuroscience* (MIT, Cambridge, MA, 2007).

[22] The map $R[\Phi] \in [0,1]$ is defined via $R[\Phi_k] = \Phi_{k+1}$. Fixed points $R[\Phi^*] = \Phi^*$ are asymptotically stable for $|R'| < 1$, unstable for $|R'| > 1$, and marginally stable if $|R'| = 1$ when R' denotes the map's derivative with respect to Φ.

[23] Y. Tsubo *et al.*, Eur. J. Neurosci. **25**, 3429 (2007).